PPPL-1922

UC20-A,G

I-6039

PPPL-1922

Dr. 935

MASTER

ANALYSIS OF THE PLASMA SWEEPER

By

J. Glanz and R.W. Motley

SEPTEMBER 1982

PLASMA PHYSICS LABORATORY

PRINCETON UNIVERSITY

PRINCETON, NEW JERSEY

PREPARED FOR THE U.S. DEPARTMENT OF ENERGY,
UNDER CONTRACT DE-AC02-76-CHO-3073.

DISTRIBUTION OF THIS DOCUMENT IS UNLIMITED.

NOTICE

This report was prepared as an account of work sponsored by the United States Government. Neither the United States nor the United States Department of Energy, nor any of their employees, nor any of their contractors, subcontractors, or their employees, makes any warranty, express or implied, or assumes any legal liability or responsibility for the accuracy, completeness or usefulness of any information, apparatus, product or process disclosed, or represents that its use would not infringe privately owned rights.

Printed in the United States of America.

Available from:

National Technical Information Service
U. S. Department of Commerce
5285 Port Royal Road
Springfield, Virginia 22151

Price: Printed Copy $ * ; Microfische $3.50

*PAGES	NTIS Selling Price
1-25	$5.00
26-50	$6.50
51-75	$8.00
76-100	$9.50
101-125	$11.00
126-150	$12.50
151-175	$14.00
176-200	$15.50
201-225	$17.00
226-250	$18.50
251-275	$20.00
276-300	$21.50
301-325	$23.00
326-350	$24.50
351-375	$26.00
376-400	$27.50
401-425	$29.00
426-450	$30.50
451-475	$32.00
476-500	$33.50
500-525	$35.00
526-550	$36.50
551-575	$38.00
576-600	$39.50

For documents over 600 pages, add $1.50 for each additional 25 page increment.

PPPL--1922

DE83 001392

Analysis of the Plasma Sweeper

J. Glanz and R. W. Motley

Plasma Physics Laboratory, Princeton University
Princeton, New Jersey 08544

ABSTRACT

The coupling of lower hybrid waves to a plasma can be modified by placing potentials on electrodes near the mouth of a phased array. Positive potentials on the electrodes create an electric field that sweeps the plasma away at a velocity $c\,\bar{E}\times\bar{B}/B^2$. In this paper we derive the electric field created by the applied potential from the nondivergent character of the current flow and the ion momentum equation, in which ion-neutral charge-exchange collisions are retained, and we compare the predictions with experimental data.

DISCLAIMER

This report was prepared as an account of work sponsored by an agency of the United States Government. Neither the United States Government nor any agency thereof, nor any of their employees, makes any warranty, express or implied, or assumes any legal liability or responsibility for the accuracy, completeness, or usefulness of any information, apparatus, product, or process disclosed, or represents that its use would not infringe privately owned rights. Reference herein to any specific commercial product, process, or service by trade name, trademark, manufacturer, or otherwise, does not necessarily constitute or imply its endorsement, recommendation, or favoring by the United States Government or any agency thereof. The views and opinions of authors expressed herein do not necessarily state or reflect those of the United States Government or any agency thereof.

DISTRIBUTION OF THIS DOCUMENT IS UNLIMITED

A. INTRODUCTION

The plasma sweeper, a device intended to modify the coupling properties of RF waveguides, has been presented in a previous paper and its basic operational properties discussed [1]. It owes its possible utility to the fact that in overdense plasmas ($\omega_{pe}^2 >> \omega^2$, where ω_{pe} is the electron plasma frequency and ω is the wave frequency) the reflective properties of waveguides operating in the lower hybrid regime of frequencies are essentially determined in the narrow layer near the edge of the plasma, in which $\omega_{pe}^2 \approx \omega^2$. Density modifications in this critical region may correspondingly have a strong effect on the reflection. Thus, we showed previously that the insertion of two thin carbon limiters or wings significantly altered the backward-coupled power ~ 100 μsec after the application of a positive bias (40 V). Plasma density in the critical region was reduced on the same time-scale by a vertical $\underline{E}\times\underline{B}$ drift at ~1/2 C_s, where C_s is the sound speed. Equations governing the penetration of the electric field across field lines into the plasma (on a scale of ~1 cm, much larger than both the Debye length and the ion-cyclotron radius) were not given, however.

In the present work we study the detailed physics of the sweeper. (See Fig. 1 for sweeper schematic.) It is known from the experiments of Okabayashi and Yoshikawa [3], and of Strait [4] that ion collisions with neutral particles can cause cross-field current flow; by balancing this current

with collisionless flow along field lines, a nonlinear equation for the potential is developed and solved. The solutions (for positive potentials) are first compared with an experiment when density gradient effects are neglected; density gradients are subsequently added to the analysis. In Sec. D we show that the charge drawn to the biased limiters is primarily due to current flowing across field lines and can exceed 1A under typical conditions. Finally, the question of negative potentials is considered.

The measurements were performed in the H-1 linear test plasma [5] with typical operating parameters: plasma density $n \sim 5 \times 10^{11}$ cm^{-3}, electron and ion temperatures $T_e \sim 1$ eV, $T_i < 1$ eV, neutral pressure $p \sim 0.4$ mT and axial magnetic field $B \leq 15$ kG. Most of the data were taken in argon plasmas, with some in helium and neon. Time scales of the experiment were short compared with the decay time (~1 ms) of the afterglow plasma. The waveguide-sweeper apparatus was positioned some variable distance into the gradient at the plasma edge, and halfway between the conducting end plates (end plate separation $\tau = 270$ cm). Floating potential measures were obtained using a wire probe and a "bridge" circuit, so that the current to the probe could be manually adjusted to zero at each point in space. The probe entered from a port opposite the waveguide and could be extended and retracted along different chords.

We remark that the basic configuration of the sweeper may in particular have application in tokamak wave-heating

experiments, in which the plasma density outside the waveguide mouth is frequently too high for efficient coupling. Other schemes in which static E-fields are applied at the edge of a plasma, (mainly in toroidal devices to control impurities), have been proposed in the literature [6-9].

B. EQUATION FOR THE POTENTIAL

An equation for the potential may be derived from the condition of zero charge accumulation:

$$\nabla \cdot \underline{J} = 0 \quad . \tag{1}$$

We will compute the currents in the idealized geometry of Fig. 2. The plasma is assumed to extend infinitely away from the limiters (except in the x-direction where the plasma density approaches zero), and vertical variation is neglected; the limitations of these assumptions are discussed in part in Sec. C. From the ion fluid momentum equation, the cross-field current may be expressed in terms of the electric field [9]:

$$nm_i \frac{\partial \underline{v}}{\partial t} + nm_i \underline{v}\cdot\nabla\underline{v} + \kappa T_i \nabla n + en\nabla\phi - \frac{e}{c} n\underline{v} \times \underline{B} = - \nu nm_i \underline{v} \ .$$

Charge-exchange collisions between ions and atoms will produce the principal contribution to ν, the "collision frequency." The potential ϕ is measured with respect to ground, and m_i is the ion mass. Ion pressure effects will be neglected here and considered in the Appendix; $\frac{\partial}{\partial t} \equiv 0$ in our geometry; the

convective derivative is seen to be negligible a posteriori. Since $\omega_c 2 >> \nu^2$ for B > 2.5 kG under all conditions of the experiment we find for the current

$$J_x = - en \frac{\nu C_s^2}{\omega_c^2} \frac{\partial \psi}{\partial x} \quad . \tag{2}$$

In this equation $C_s^2 = \kappa T_e/m_i$, the cyclotron frequency $\omega_c = eB/m_i C$, and $\psi = e\phi/\kappa T_e - \ell n\ (m_i/m_e)$. Electron current in this direction is of order m_e/m_i in comparison and $J_y = 0$ to first order in ν/ω_c.

Equation (1) may be integrated from endplate-to-endplate along a magnetic field line (up to the "sheath edges") and the Langmuir relation (obtainable from Bohm's arguments [10]) applied:

$$J_z(L/2) = - J_z(-L/2) = enC_s(1 - e^{-\psi}) \quad . \tag{3}$$

Combining the result with Eq. (2), we find:

$$\frac{1}{n} \frac{\partial}{\partial x}(n \frac{\partial \psi}{\partial x}) = \frac{1}{\delta^2} (1 - e^{-\psi}) \qquad (x > 0) \tag{4}$$

$$\delta = \frac{1}{\omega_c} \left(\frac{\nu C_s L}{2} \right)^{1/2} .$$

In deriving this equation we have made a "uniformity hypothesis," neglecting the z-variation of J_x in the integration. This can be justified using the full differential equation before integration; the comparatively large conductivity along field lines

manifests itself in elongated potential structures. We checked this prediction directly with an axial probe during the experiment and found it to hold.

Equation (4) is our basic relation. It expresses the fact that whenever the potential deviates from its ambipolar value, a transverse gradient must arise to drive current across field lines.

It is illuminating to study the solutions to this equation in a uniform plasma, where it admits of one exact integral:

$$\frac{\partial \psi}{\partial x} = \frac{-2^{1/2}}{\delta} \left(\psi - 1 + e^{-\psi}\right)^{1/2} . \qquad (5)$$

ψ and its derivative have been prescribed to be zero at infinity. When ψ is small, $e^{-\psi}$ may be expanded. The solutions are decreasing exponentials with e-folding length δ, so that any solution has an exponential tail. For ψ large and positive the $e^{-\psi}$ term is unimportant, and the solutions are parabolic to lowest order:

$$(\psi)_o = 1 + \frac{1}{2} u^2,$$

where $u = 2^{1/2} (\psi_o - 1)^{1/2} - x/\delta$, and ψ_o is the (exact) value of ψ at $x = 0$. Higher-order solutions can be computed by formally ordering $e^{-(\psi)_o}$ as a small parameter and expanding both the square root and the exponential itself, in Eq. (5), in accordance with this ordering. Alternatively, a far simpler procedure is to construct a global matched solution. We here state the result of such a procedure:

$$\psi \simeq \begin{cases} 1 + u^2/2 & (u > \sqrt{2}) \\ 8/3\ e^{(u-\sqrt{2})} - 2/3\ e^{2(u-\sqrt{2})} & (u < \sqrt{2}). \end{cases} \qquad (6)$$

When compared with numerical solutions of Eq. (5), this approximation gives "width-of-line" (<5%) accuracy over the entire range. If $\psi_o \leq 2.0$, only the small ψ solutions need be used.

The case of ψ large and negative is of importance only if the sweeper emits electrons. Negative potentials (from non-emitting electrodes) are considered in Sec. E.

We may note that Eq. (5) is identical to the Debye shielding equation (with stationary ions and Boltzmann electrons) with the Debye length replaced by δ. The problems are distinct, however. For example, ours is a quasi-neutral "sheath."

C. POSITIVE POTENTIALS

The simplest prediction of Eq. (5) is that the electric field should be proportional to δ^{-1} (at a given potential), which varies as B and $p^{-1/2}$. This general behavior is evident in Fig. (3). ($\bar{\delta}$ is the inverse slope of the curves at $\psi \simeq 2$, an easier quantity to measure experimentally. In our previous paper, this quantity was called δ.) The rise in the experimental points near x = 0 results from the density fall-off in front of the electrodes and is discussed in the next section. The slopes in Fig. (3) may be catalogued and plotted vs 1/B [Fig. (4)]. Deviations at the largest δ's (δ > 5 cm) are

expected because the assumption of finite geometry becomes invalid. Finite geometry would spread the profiles out somewhat, since the actual condition at the plasma edge will be one of zero slope in potential (zero current flow). If a number of graphs such as Fig. (4) are collated, the pressure dependence of Fig. (5) emerges.

The $m_i^{1/2}$ dependence of δ has been verified in helium and neon discharges. We also verified the independence of δ on plasma density (over a factor of 5 in density with neutral pressure constant).

In the theoretical analysis we have assumed the charge-exchange frequency to be due primarily to axial flow:

$$\nu \simeq N\sigma C_s ,$$

where N is the neutral density and σ is the cross section [11],

$$\sigma \simeq 6.0 \times 10^{-15} \text{ cm}^2 \text{ at } T_e \simeq 1 \text{ eV in Ar.}$$

To obtain the absolute agreement, it has been necessary to multiply the reading of our ionization pressure gauge by 7.0 . This yields the numerical form of δ:

$$\delta \simeq .49 \frac{(A\, p\, T_e)^{1/2}}{B} ,$$

where A is the atomic number.

Eq. (6) predicts a transition from the exponential solution in its nonlinear regime [not very evident in Fig. (4) because

of the size of the potentials]. Figure (6) shows that the nonlinear solutions are found experimentally. According to Eq. (5), in the absence of density gradients the maximum electric field should go as $\phi_\ell^{1/2}$ in this regime, where ϕ_ℓ is the limiter potential measured with respect to ground. We verify this dependence in Fig. (7). The expected dependencies of E_{max} on pressure and magnetic field are also recovered in the experiment.

The electric fields should drive a plasma $\underline{E}\times\underline{B}$ drift. The drift can readily be observed, since $\nabla n \neq 0$, and it is of the correct magnitude to within ~ 50%. Since $E \propto B$, the $\underline{E}\times\underline{B}$ drift should be independent of B, as seen in Fig. 8.

Plasma drifts will distort the radial profile as seen in Fig. 9. The ultimate edge of the plasma can be at a substantial remove from the limiters in the case of low field and high voltage. Such distortions will, in turn, affect the reflectivity of the waveguide, as shown in Ref. 1.

D. EFFECT OF THE DENSITY GRADIENT

The analysis given in Sec. B is incomplete in that there will always be gradients near the edge of the plasma. In this section we include them in an idealized, exponential form (although the problem as we shall state it, is solvable in quadrature for arbitrary gradients). The justification for the idealized gradient is that only strong gradients can affect the potential profiles much for moderate B-fields. At low fields more realistic profiles may be necessary.

The density, then, is to be of the form:

$$n(x) = \begin{cases} n_o e^{\lambda(x-x_o)} & (x < x_o) \\ n_o & (x > x_o) \end{cases} .$$

The limiters extend to x = 0. We further specialize to the case, easiest to measure, in which $\psi_o > 2.0$. The limiters are supposed to impress the (normalized) potential ψ_o on the plasma at $x = x_o \leq 0$. Analytic approximations similar to those of Sec. B can be derived:

$$\psi = \begin{cases} \psi_1(x) & (-x_o < x - x_o < 0) \\ \psi_2(x) & (\sqrt{2}(B-1)\delta > x - x_o > 0) \\ \psi_3(x) & (x - x_o > \sqrt{2}(B-1)\delta) \end{cases} ,$$

$$\psi_1(x) = \psi_o + \frac{1}{\lambda}(1-e^{-\lambda x})S' + \frac{1}{\delta^2\lambda}\left[x + \frac{1}{\lambda}(e^{-\lambda x} - 1)\right],$$

$$\psi_2(x) = 1 + \left(S - \frac{x-x_o}{\sqrt{2}\delta}\right)^2 ,$$

$$\psi_3(x) = \frac{8}{3}\exp\left[\sqrt{2}\,(S-1) - \frac{(x-x_o)}{\delta}\right] - \frac{2}{3}\exp\left[2\sqrt{2}\,(S-1) - 2\,\frac{(x-x_o)}{\delta}\right] ,$$

$$S' = \frac{1}{\delta}\left[\frac{1}{\alpha^2}\left(\frac{\lambda x_o^2}{\delta}\right) - e^{\lambda x_o}\sqrt{2(\psi_o - 1 + \bar{\psi})}\right] ,$$

$$S = \frac{1}{\alpha}\left(\frac{-x_o}{\sqrt{2}\,\delta}\right) + \sqrt{\psi_o - 1 + \bar{\psi}} ,$$

$$\alpha = \frac{\lambda x_o e^{-\lambda x_o}}{1 - e^{-\lambda x_o}} ,$$

$$\bar{\psi} = \frac{1}{\delta^2\lambda^2}\left[\lambda x_o + \frac{1}{2}\left(e^{\lambda x_o} - 1\right)\left(e^{\lambda x_o} - 3\right)\right] .$$

An increasing gradient causes a faster falloff in potential, because the charge to alleviate the drain out the ends of a given field line comes from lower density regions, or regions with fewer charge carriers. The theory is plotted with points in Fig. (10); the gradual bulge in the density profile, left out of the model, is evidently unimportant.

E. CURRENT TO THE LIMITERS

The problems considered here are relevant in determining the current collected by a biased conducting object in a magnetized plasma, in the presence of a non-zero cross-field conductivity. One shows, for example, using Eq. (1) as before and the solutions of the previous section with $\psi_\ell \equiv e\phi_\ell/\kappa T_e \simeq \psi_o >> 1$ and $x_o \simeq 0$, that the net current into both limiters is given by

$$I_\ell \simeq 2en(0)C_s\, h\left[\delta\sqrt{2\,\psi_\ell - 1}\right) + \int_{-\infty}^{0}\frac{n(x)}{n(0)}\,dx\,\Big]$$

$$\simeq 2en(0)C_s\, h\,\delta\sqrt{2(\psi_\ell - 1)} \quad , \qquad (7)$$

where h = 6.5 cm is the height of the limiters. The retained term is due to cross-field current flow usually much larger (~×10) than the current flow along field lines occuring when no neutral

atoms are present. For $n(0) \sim 3 \times 10^{11}$ cm^{-3}, $T_e \sim 1$ eV, $\delta \sim 1$ cm, $\psi_\ell \sim 1$ V, we have $I_\ell \sim 1$A. Measurements of I_ℓ show that collection current up to 2A can be drawn across field lines. Fig. (11) shows the time-variation of the current. Following an initial peak, the current drops as the plasma in front of the limiters is depleted. I_{max} is compared with Eq. (7) in the next two figures. The saturation in I_ℓ of Fig. (13) may be caused by a reduction in the E-fields by finite geometry. There is also some change in the density profiles with magnetic field, which has not been taken into account.

The large currents originating in cross-field flow may be of importance in tokamak experiments (with suitable alterations in the theory). On PLT and PDX, large currents (> 100A) were drawn when the limiters were biased positively.

F. NEGATIVE POTENTIALS

In all of the previous studies we have treated the limiters merely as imposing a boundary condition on ψ. This is not strictly true; however, when $\psi_\ell > 0$, the potential in the shadow of the sweeper is approximately the same as the applied potential because of the high mobility of the electrons. The situation alters for $\psi_\ell < 0$, when the charge must be drained by ions moving at the sound speed. The current flow parallel to B may not be as large as $J_x hL$, so that the

plasma potential is normally much less than the applied potential, to prevent the overflow.

A theory may be formulated to give the plasma potential, in which the plasma is cut off a distance D behind the limiters; no current is to flow past this ledge in density. To first order in D/δ quantities involving the (assumed exponential) density gradient drop out, and one obtains for the potential at $x = 0$

$$\psi_\ell \simeq \frac{-D}{\delta} (1 - e^{\psi_\ell}) \quad .$$

The linearity with B is found experimentally (Fig. 14) . To coincide in magnitude with the theory, one must set D = .36 cm, about twice the gradient e-folding length at the time the measurements were taken. This value of D has then been applied to the curve of Fig. (15).

To conclude, we have shown that electric fields arising from potentials applied at the edge of a linear plasma can be explained by balancing collisionless current flow along field lines with cross-field flow due to charge exchange between ions and neutral atoms. The results are of relevance to waveguide coupling experiments, in which the electric fields would modify density profiles at the plasma edge. Further, these effects must be taken into account in determining the current collected by biased conducting objects in a magnetized plasma (e.g., probes or limiters).

G. APPENDIX (VISCOSITY)

Because there is velocity shearing predicted by Eq. (4), the addition of finite gyroradius terms to the pressure tensor will correct the overall solution, even in the absence of density gradients. This correction is straightforward to obtain once the pressure tensor is known. Its elements, in our case, will themselves be modified by the presence of background neutrals. We have calculated these modifications using the simplified method of Kaufmann[12] in which we insert a second Krook collision operator into the Boltzmann equation to account for ion-neutral charge-exchange collisions. When there are no plasma gradients (the case considered here), such corrections drop out when the divergence of the pressure tensor is taken. From the ion momentum equation, one then finds for the x-current

$$J_x = - en \frac{\nu C_s^2}{\omega_c^2} \frac{\partial}{\partial x} \left(\psi - \delta_i^2 \frac{\partial^2 \psi}{\partial x^2} \right) , \qquad (8)$$

$$\delta_i^2 = \frac{\mu_o}{\nu m_i n_e} \frac{1}{1+4(\omega_c \tau_{ii})^2} .$$

Here, $\tau_{ii} = \mu_o / ne \kappa T_i$ is the ion self-collision time, and μ_o is the classical coefficient of viscosity:

$$\mu_o = (5/8\pi^{1/2})(m^{1/2}(\kappa T_i)^{5/2}/e^4 \ln \Lambda),$$

Under our conditions $\ln \Lambda \simeq 10$.

A more complicated equation, analogous to Eq. (5), is obtained for the potential:

$$\delta_i^2 \left[\frac{\partial \psi}{\partial x} \frac{\partial^3 \psi}{\partial x^3} - \frac{1}{2} \left(\frac{\partial^2 \psi}{\partial x^2} \right)^2 \right] - \frac{1}{2} \left(\frac{\partial \psi}{\partial x} \right)^2 + \frac{1}{\delta^2} (\psi - 1 + e^{-\psi}) = 0. \tag{9}$$

We discuss this equation only in the limit that the Boltzmann factor is negligible (when ψ is small it is, of course, equivalent to a linear equation). By educated guessing and substitution one can show that in this limit the following three-parameter solution holds:

$$\psi = 1 + \frac{\delta_i^2}{2\delta^2} [1 + (x/\delta_i + A)^2] + B e^{-x/\delta_i} + C (4 + \frac{1}{B} e^{x/\delta_i}), \tag{10}$$

where A, B, and C are arbitrary constants. We may reasonably set C = 0; one more constant is fixed by the fin potential; the final must depend on how the boundary at x = 0 is treated with respect to plasma flow. Two possible choices are free-slip and no-slip, and we have chosen the former as there is no corporeal "wall" at x = 0; this overlooks any drag effected by the plasma in the region x < 0. The free-slip condition implies that all bulk stresses must vanish at x = 0, namely, that the (1,2) component of the pressure tensor must vanish at this point. The (1,2) component is proportional to the second spatial derivative of the potential.

Proceeding from Eq. (10), these considerations produce the solution:

$$\psi = \left(1 + 2\,\frac{\delta_i^2}{\delta^2}\right) + 2\left[x + \sqrt{\tfrac{1}{2}(\psi_o - 1) + \delta_i^2/\delta_o^2}\right]^2 - 4\,\frac{\delta_i^2}{\delta_o^2}\,e^{-x/\delta_i}\,, \qquad (11)$$

ψ_o is the value of the potential at x = 0.

Since, in our typical situation, δ_i^2/δ_o^2 is very small, the addition of viscosity will not have a great impact on the overall solution. A plot of the ratio is given in Fig. (17). This ratio is larger and can approach unity at our lowest neutral pressures and electron temperatures; however, even there the character of the nonlinear solution tends to "downplay" the viscous effects. Moreover, we observe no strong evolution of the profiles in these circumstances.

ACKNOWLEDGMENTS

We gratefully acknowledge the technical assistance of J. Frangipani, who constructed the plasma sweeper.

This work has been supported by the U.S. Department of Energy Contract No. DE-AC02-76-CHO3073.

REFERENCES

[1]R. W. Motley and J. Glanz, to be published in Phys. Fluids.

[2]M. Brambilla, Nucl. Fusion 16, 47 (1976).

[3]M. Okabayashi and S. Yoshikawa, Phys. Rev. Lett. 29, 1725 (1972).

[4]E. J. Strait, Nucl. Fusion 21, 943 (1981).

[5]R. W. Motley, S. Bernabei, W. M. Hooke, and D. L. Jassby, J. Appl. Phys. 46, 3286 (1975).

[6]S. I. Braginskii, Fiz. Plazmy 1, 370 (1975); Sov. J. Plasma Phys. 1, 202 (1975).

[7]T. Consoli, R. LeGardeur, G. F. Tonon, in Plasma Physics and Controlled Nuclear Fusion Research, Proc. 5th International Conference, Tokyo, 1974, Vol. 1 (IAEA, Vienna, 1975) p. 571.

[8]E. J. Strait, D. W. Kerst, and J. C. Sprott, Phys. Fluids 21, 2342 (1978).

[9]L. Spitzer, Physics of Fully Ionized Gases, Second Edition, Interscience, New York (1962) p. 158.

[10]D. Bohm, The Characteristics of Electrical Discharges in Magnetic Fields, edited by A. Guthrie and R. K. Wakerling, McGraw-Hill, New York (1949) Ch. 2 (Sec. 4), and Ch. 3.

[11]S. Brown, Basic Data of Plasma Physics, Second Edition, M.I.T. Press, Cambridge (1966) Ch. 3.

[12]A. N. Kaufman, Phys. Fluids 3, 610 (1960).

FIGURE CAPTIONS

Fig. 1. Schematic of the Sweeper. Diameter of plasma column is 10 cm, and the height of the sweeper electrodes 6.5 cm; each electrode is separated from the nearest guide by 6.7 cm.

Fig. 2. Idealized geometry of Sec. B. The plasma extends infinitely in the y-direction and in the positive x-direction; in the negative x-direction the density eventually goes to zero due to gradients. x=0 marks the limiter edge in this and all graphs.

Fig. 3. A set of potential curves compared with theory. $T_e \approx 1.0$ eV for all the curves; $n_e \approx 2 \times 10^{11}$ cm^{-3} at the lower, and $n_e \approx 8 \times 10^{11}$ cm^{-3} at the higher pressure. Plasma gradients extend somewhat more deeply at the lower magnetic fields but otherwise the parameters do not change with field. (Measurements obtained on midplane.)

Fig. 4. Summary of a number of potential profiles. $\bar{\delta}$ is the inverse slope at $\psi \approx 2$.

Fig. 5. Collation of the slopes of graphs as in Fig. 4. P is the background pressure of neutrals.

Fig. 6. Graph showing the nonlinear solutions to the potential. $p = 5.0 \times 10^{-4}$ T.

Fig. 7. Dependence of the maximum electric field, E_{max}, on the limiter potential, ϕ_ℓ, in the nonlinear regime. $p \approx 5.0 \times 10^{-4}$T.

Fig. 8. Plasma drift velocity (in a direction parallel to the limiter edges) as the magnetic field is changed.

Fig. 9. Radial density profiles on midplane as the plasma moves away from the limiter edges. A + 30 V potential is applied at the zero of time; B = 4.0 kG and p = 5.0×10^{-4}T.

Fig. 10. Comparison with Eq. 4 when a simplified density gradient is taken into account. The gradual bulge between x = 1 cm and x = 2 cm in the density profile has been neglected. To accentuate the gradient effects, measurements were made 120 μs after the beginning of the pulse. The region x < .5 cm is one of very low density. B = 6.0 kG, p = 5.0×10^{-4}T.

Fig. 11. Sum of the currents to the limiters in time. B = 12.0 kG, p = 5.0×10^{-4}T.

Fig. 12. Current-voltage characteristic of the limiters. B = 4.0 kG, p = 1.0×10^{-4}T.

Fig. 13. Current to limiters as magnetic field is changed. p = 5.0×10^{-4}T, ϕ_ℓ = 15 V, $n_e \simeq 3.2 \times 10^{11}$ cm^{-3}.

Fig. 14. Maximum negative potential observed in the plasma when ϕ_ℓ = ~ 15 V. The normalized volue of D is .36 cm. $T_e \simeq 1.6$ eV, p = 3.5×10^{-4}T.

Fig. 15. Maximum negative potential observed in the plasma when ϕ_ℓ is changed. B = 12.0 kG and otherwise conditions are the same as Fig. 14.

Fig. 16. The ratio δ_i/δ plotted vs ion temperature for several values of magnetic field. $n_e = 5 \times 10^{11}$ cm^{-3}, T_e = 1.0 eV, p = 0.5 mT.

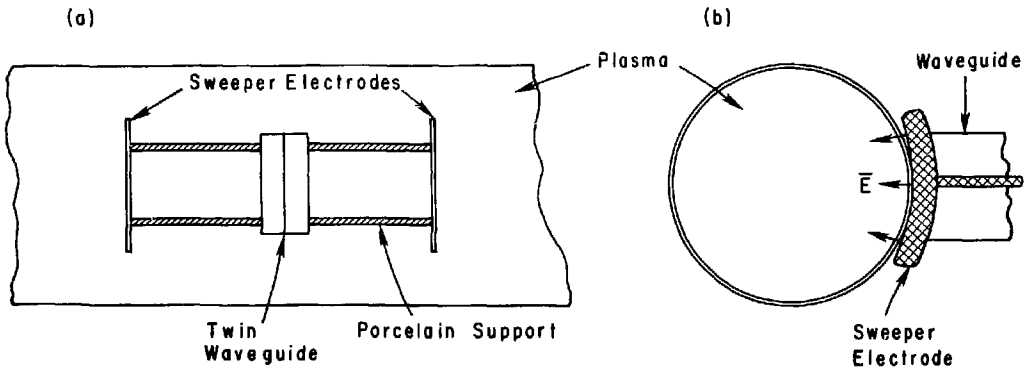
(a)
Sweeper Electrodes
Twin
Waveguide
Porcelain Support
(b)
Plasma
Waveguide
E
Sweeper
Electrode

Fig. 1

#82X0543

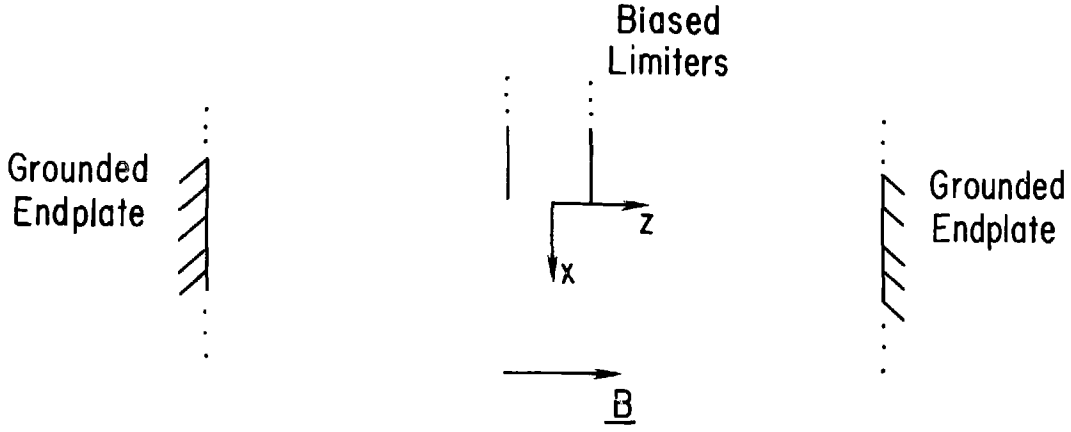

Fig. 2

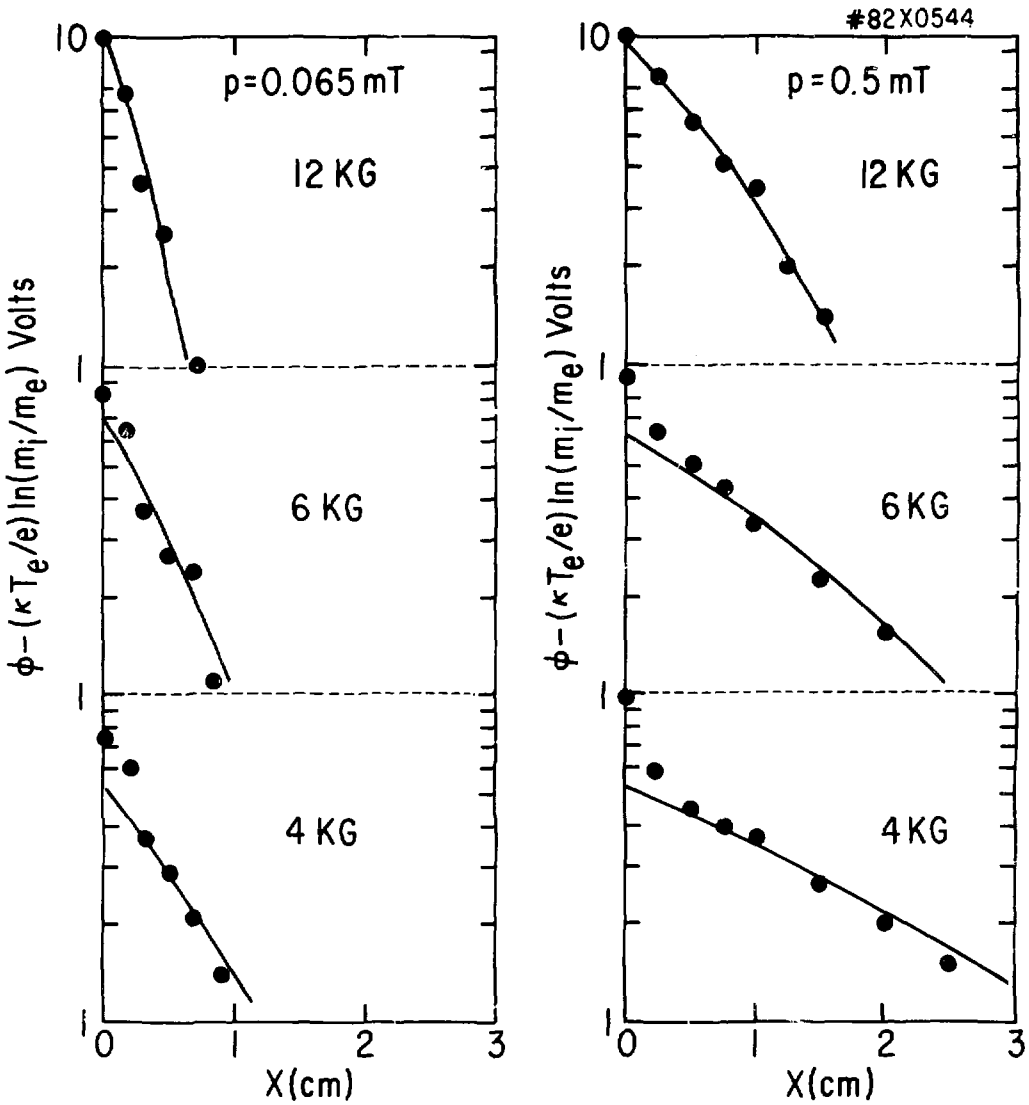
#82X0544
p=0.065 mT
12 KG
6 KG
4 KG
p=0.5 mT
12 KG
6 KG
4 KG
10
1
0
1
2
3
X(cm)
$\phi-(\kappa T_e/e)\ln(m_i/m_e)$ Volts

Fig. 3

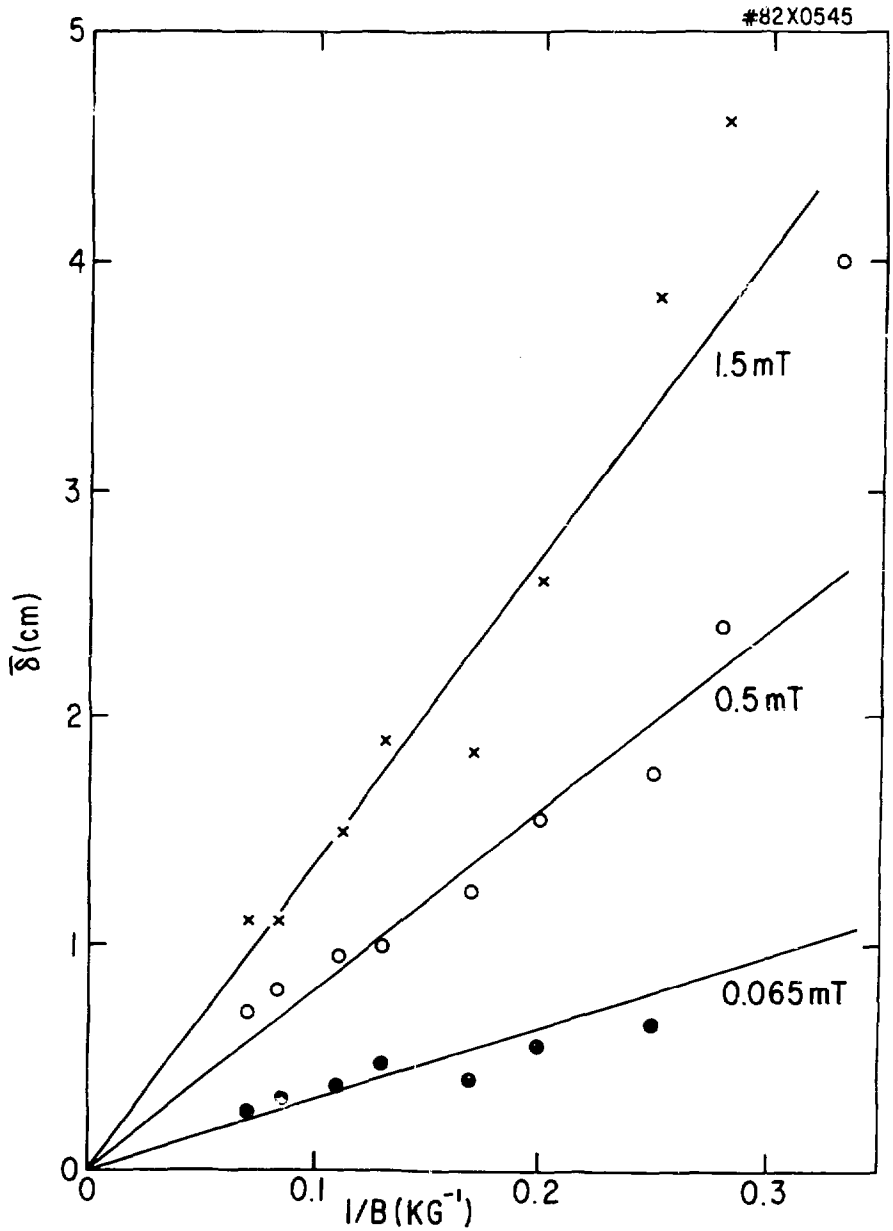

Fig. 4

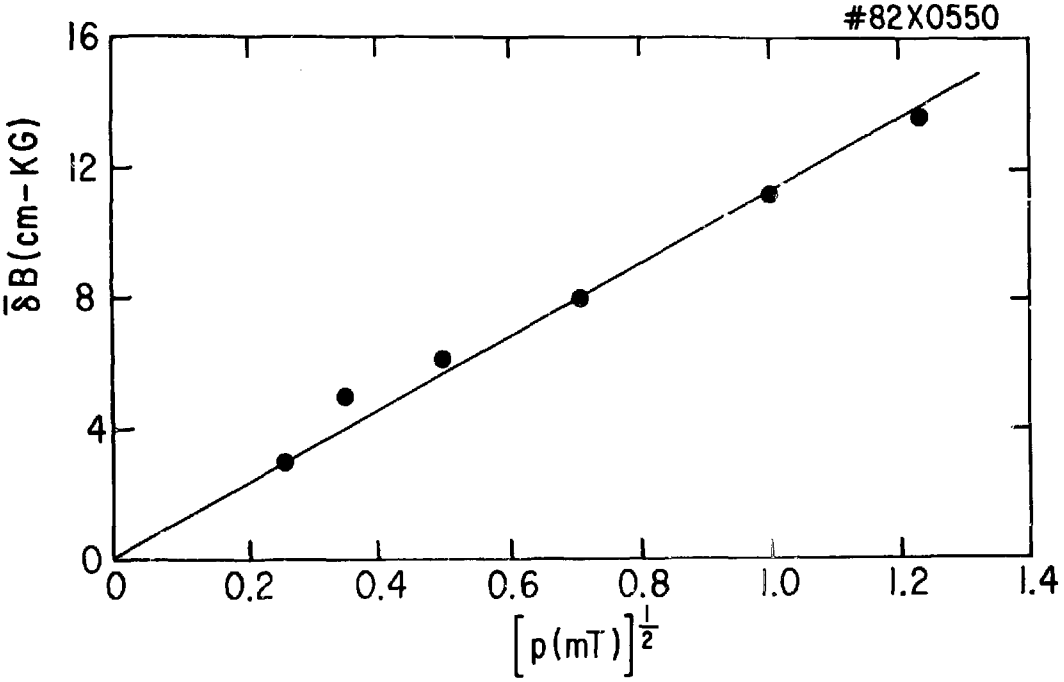
#82X0550
16
12
8
4
0
$\bar{\delta}B$(cm-KG)
0
0.2
0.4
0.6
0.8
1.0
1.2
1.4
$[p(mT)]^{\frac{1}{2}}$

Fig. 5

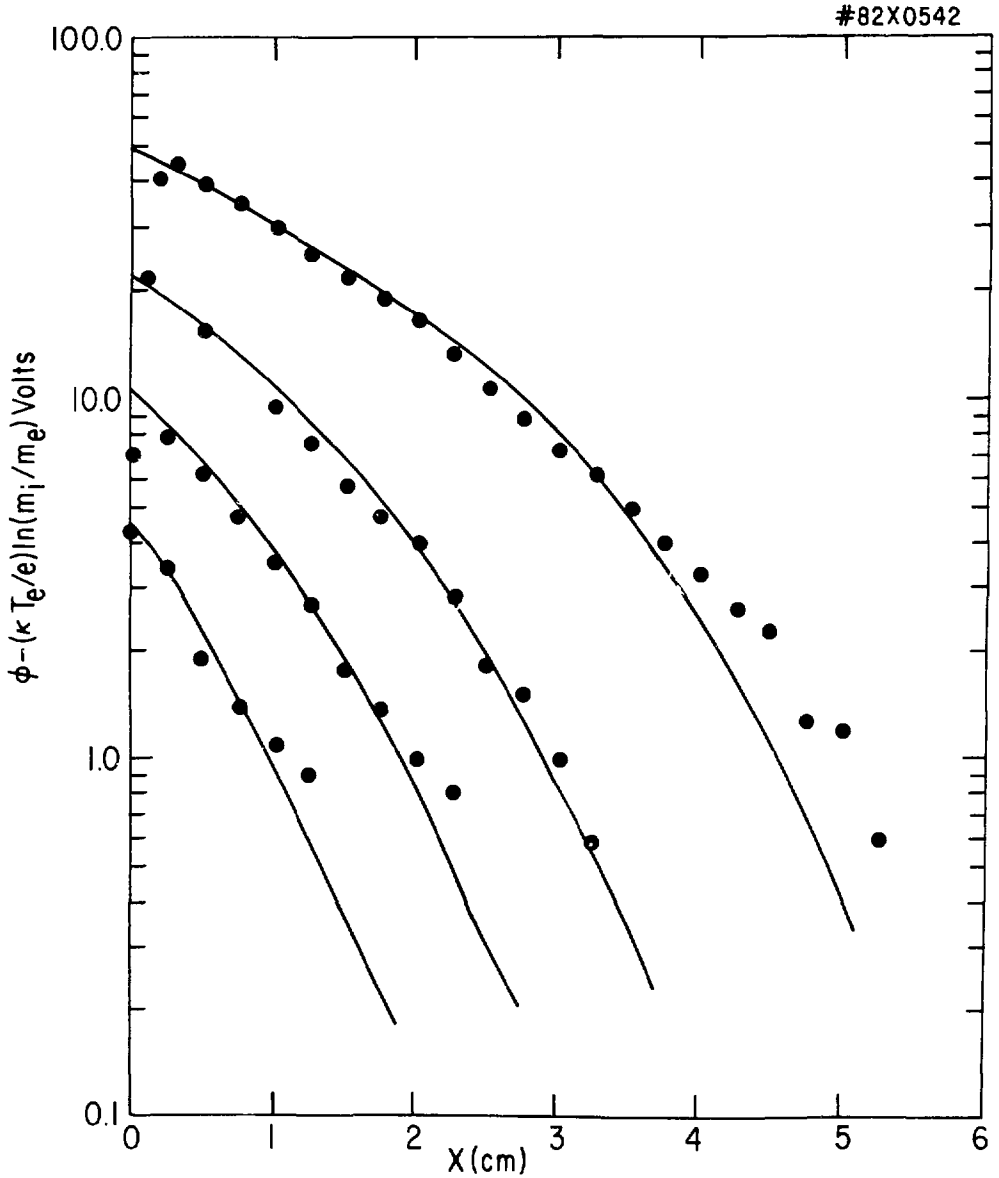
#82X0542
100.0
10.0
1.0
0.1
$\phi-(\kappa T_e/e)\ln(m_i/m_e)$ Volts
0
1
2
3
4
5
6
X(cm)

Fig. 6

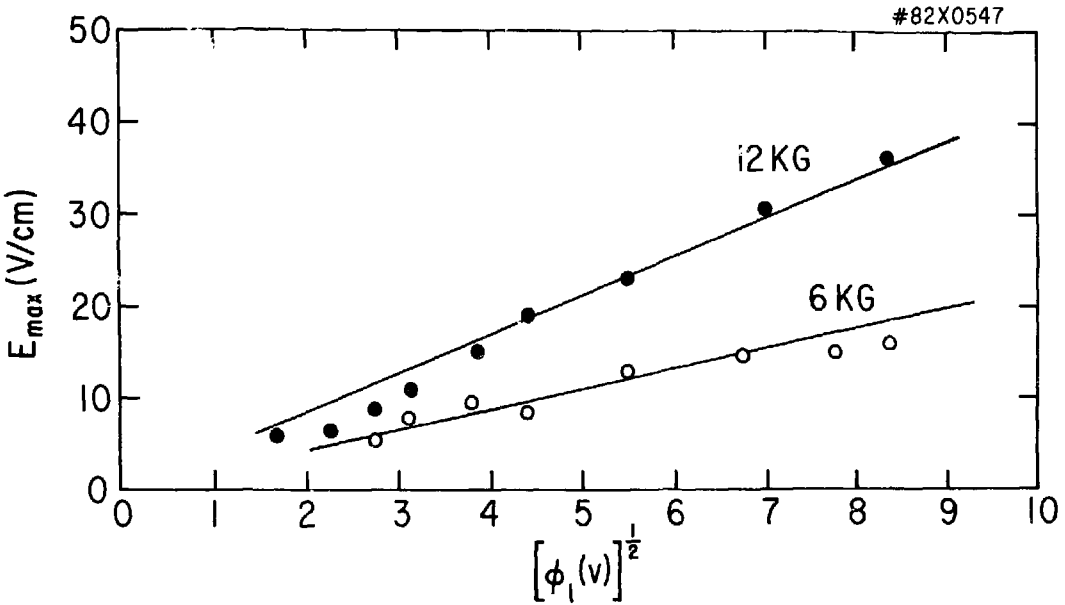
#82X0547
50
40
30
20
10
0
E_{max} (V/cm)
12 KG
6 KG
0
1
2
3
4
5
6
7
8
9
10
$[\phi_1(v)]^{\frac{1}{2}}$

Fig. 7

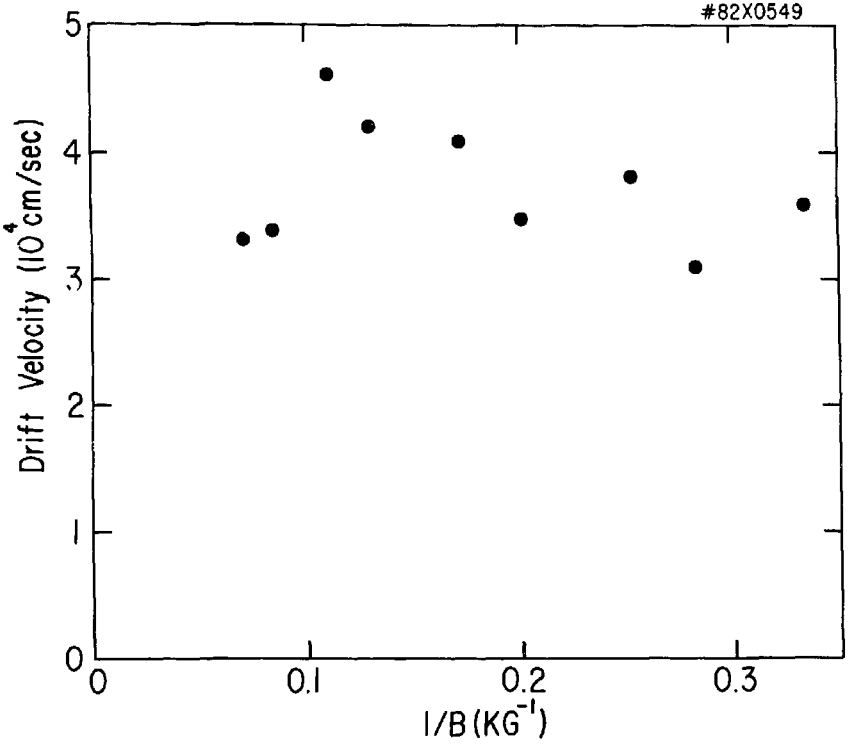

Fig. 8

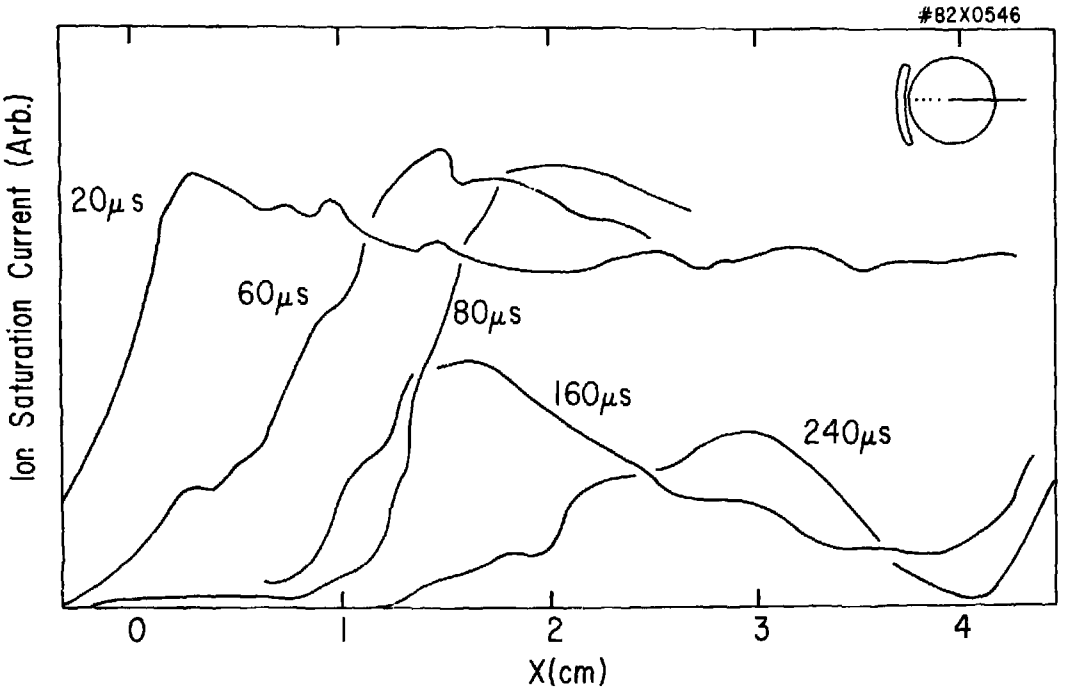
#82X0546
Ion Saturation Current (Arb.)
20μs
60μs
80μs
160μs
240μs
0
1
2
3
4
X(cm)

Fig. 9

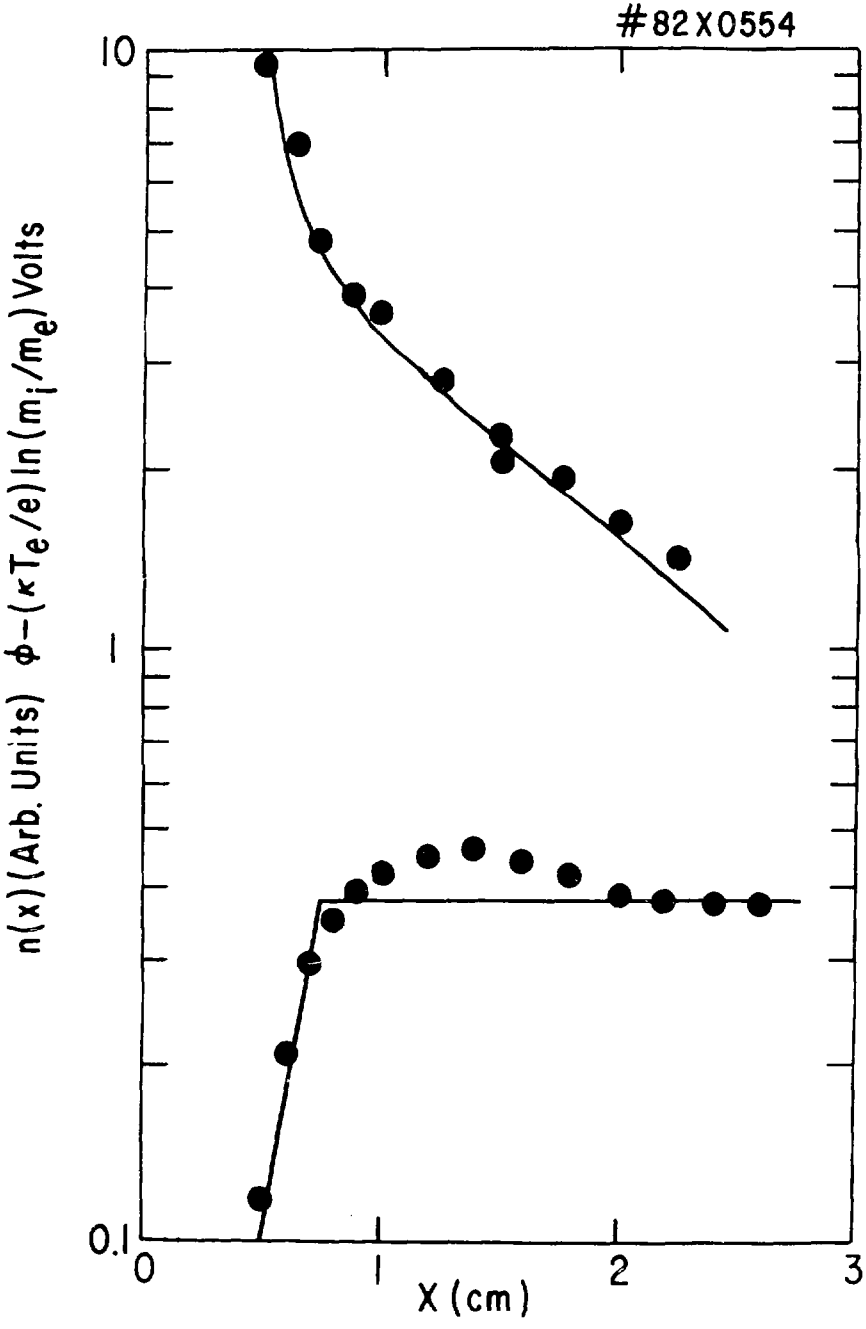
#82X0554
10
1
0.1
0
1
2
3
X (cm)
n(x) (Arb. Units) $\phi-(\kappa T_e/e)\ln(m_i/m_e)$ Volts

Fig. 10

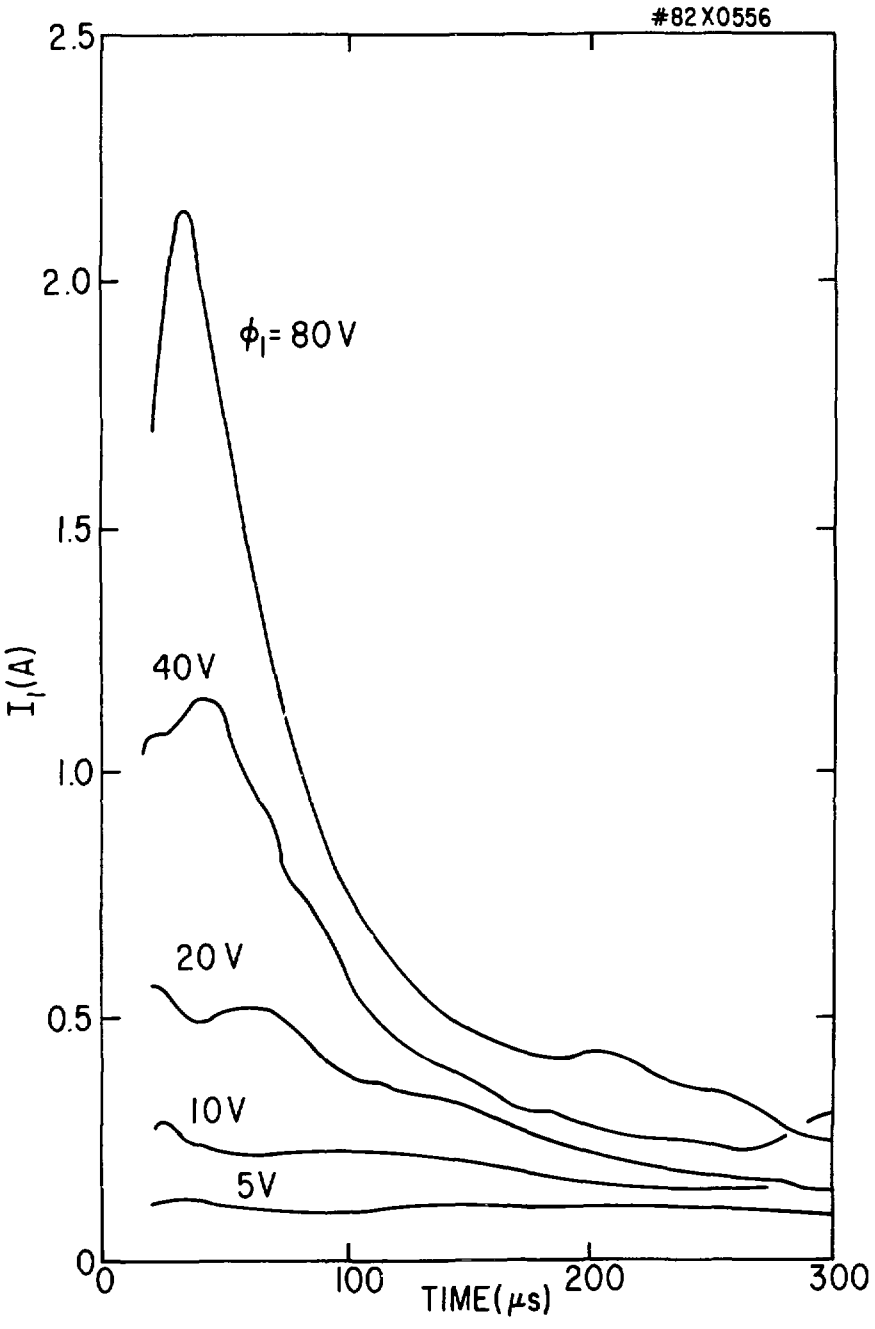
#82X0556
2.5
2.0
1.5
1.0
0.5
0
I_1(A)
ϕ_1= 80 V
40 V
20 V
10 V
5V
0
100
200
300
TIME(μs)

Fig. 11

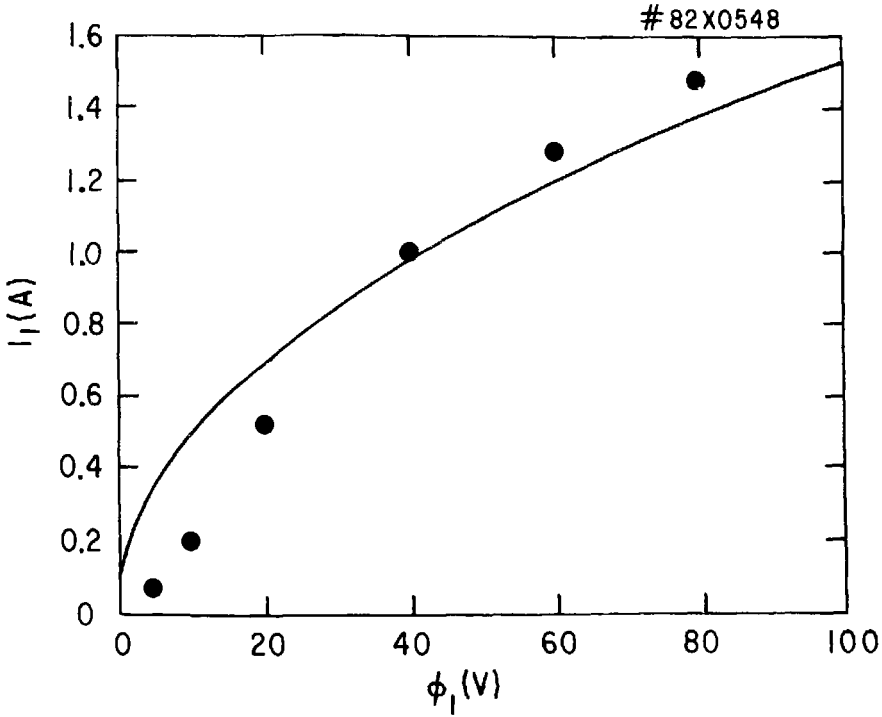

Fig. 12

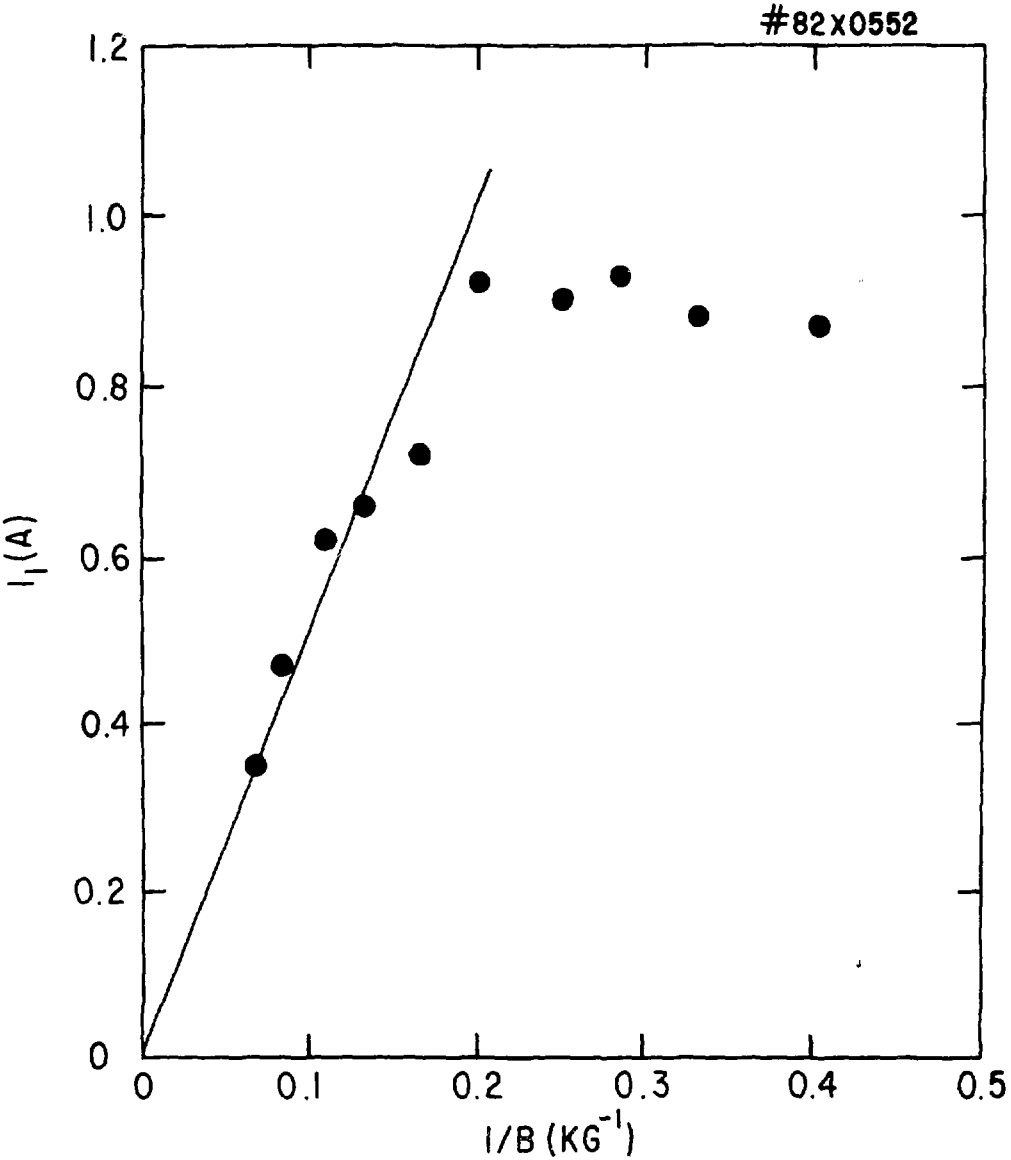

Fig. 13

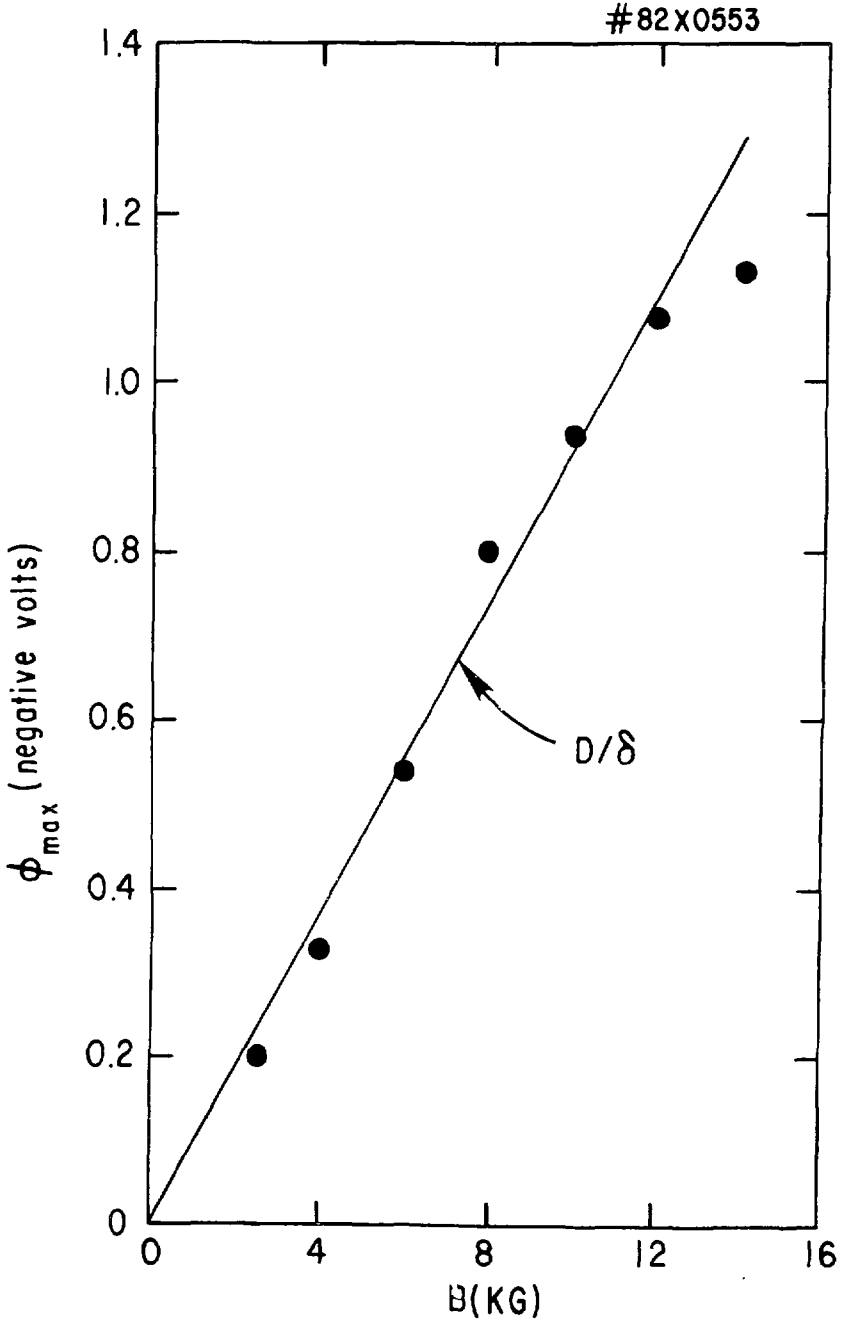
#82X0553
1.4
1.2
1.0
0.8
0.6
0.4
0.2
0
ϕ_{max} (negative volts)
D/δ
0
4
8
12
16
B(KG)

Fig. 14

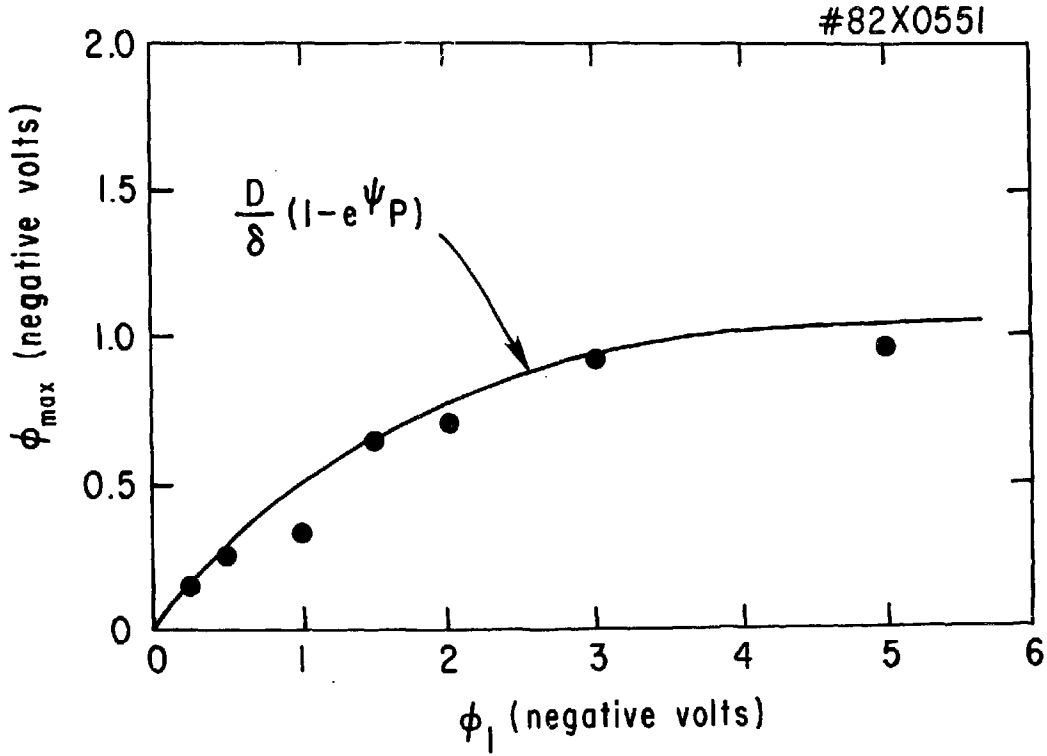
#82X0551
2.0
1.5
1.0
0.5
0
$\frac{D}{\delta}(1-e^{\psi_P})$
ϕ_{max} (negative volts)
0
1
2
3
4
5
6
ϕ_1 (negative volts)

Fig. 15

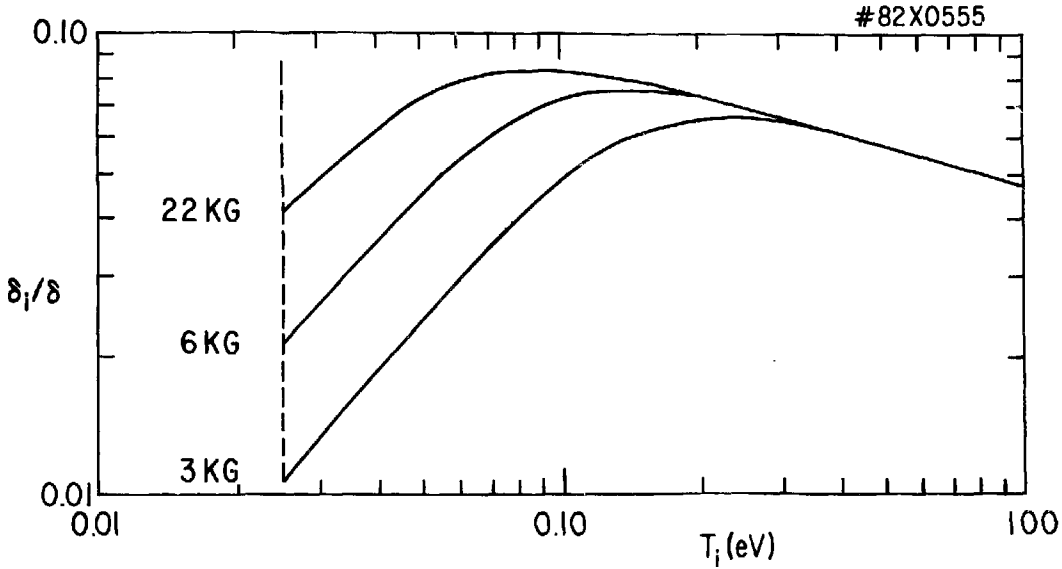

Fig. 16

EXTERNAL DISTRIBUTION IN ADDITION TO TIC UC-20

Plasma Res Lab, Austra Nat'l Univ, AUSTRALIA
Dr. Frank J. Paoloni, Univ of Wollongong, AUSTRALIA
Prof. I.R. Jones, Flinders Univ., AUSTRALIA
Prof. M.H. Brennan, Univ Sydney, AUSTRALIA
Prof. F. Cap, Inst Theo Phys, AUSTRIA
Prof. Frank Verheest, Inst theoretische, BELGIUM
Dr. D. Palumbo, Dg XII Fusion Prog, BELGIUM
Ecole Royale Militaire, Lab de Phys Plasmas, BELGIUM
Dr. P.H. Sakanaka, Univ Estadual, BRAZIL
Dr. C.R. James, Univ of Alberta, CANADA
Prof. J. Teichmann, Univ of Montreal, CANADA
Dr. H.M. Skarsgard, Univ of Saskatchewan, CANADA
Prof. S.R. Sreenivasan, University of Calgary, CANADA
Prof. Tudor W. Johnston, INRS-Energie, CANADA
Dr. Hannes Barnard, Univ British Columbia, CANADA
Dr. M.P. Bachynski, MPB Technologies, Inc., CANADA
Zhengwu Li, SW Inst Physics, CHINA
Library, Tsing Hua University, CHINA
Librarian, Institute of Physics, CHINA
Inst Plasma Phys, SW Inst Physics, CHINA
Dr. Peter Lukac, Komenskeho Univ, CZECHOSLOVAKIA
The Librarian, Culham Laboratory, ENGLAND
Prof. Schatzman, Observatoire de Nice, FRANCE
J. Radet, CEN-BP6, FRANCE
AM Dupas Library, AM Dupas Library, FRANCE
Dr. Tom Mual, Academy Bibliographic, HONG KONG
Preprint Library, Cent Res Inst Phys, HUNGARY
Dr. A.K. Sundaram, Physical Research Lab, INDIA
Dr. S.K. Trehan, Panjab University, INDIA
Dr. Indra, Mohan Lal Das, Banaras Hindu Univ, INDIA
Dr. L.K. Chavda, South Gujarat Univ, INDIA
Dr. R.K. Chhajlani, Var Ruchi Marg, INDIA
B. Buti, Physical Research Lab, INDIA
Dr. Phillip Rosenau, Israel Inst Tech, ISRAEL
Prof. S. Cuperman, Tel Aviv University, ISRAEL
Prof. G. Rostagni, Univ Di Padova, ITALY
Librarian, Int'l Ctr Theo Phys, ITALY
Miss Clelia De Palo, Assoc EURATOM-CNEN, ITALY
Biblioteca, del CNR EURATOM, ITALY
Dr. H. Yamato, Toshiba Res & Dev, JAPAN
Prof. M. Yoshikawa, JAERI, Tokai Res Est, JAPAN
Prof. T. Uchida, University of Tokyo, JAPAN
Research Info Center, Nagoya University, JAPAN
Prof. Kyoji Nishikawa, Univ of Hiroshima, JAPAN
Sigeru Mori, JAERI, JAPAN
Library, Kyoto University, JAPAN
Prof. Ichiro Kawakami, Nihon Univ, JAPAN
Prof. Satoshi Itoh, Kyushu University, JAPAN
Tech Info Division, Korea Atomic Energy, KOREA
Dr. R. England, Ciudad Universitaria, MEXICO
Bibliotheek, Fom-Inst Voor Plasma, NETHERLANDS
Prof. B.S. Liley, University of Waikato, NEW ZEALAND
Dr. Suresh C. Sharma, Univ of Calabar, NIGERIA
Prof. J.A.C. Cabral, Inst Superior Tech, PORTUGAL
Dr. Octavian Petrus, ALI CUZA University, ROMANIA
Dr. R. Jones, Nat'l Univ Singapore, SINGAPORE
Prof. M.A. Hellberg, University of Natal, SO AFRICA
Dr. Johan de Villiers, Atomic Energy Bd, SO AFRICA
Dr. J.A. Tagle, JEN, SPAIN
Prof. Hans Wilhelmson, Chalmers Univ Tech, SWEDEN
Dr. Lennart Stenflo, University of UMEA, SWEDEN
Library, Royal Inst Tech, SWEDEN
Dr. Erik T. Karlson, Uppsala Universitet, SWEDEN
Centre de Recherchesen, Ecole Polytech Fed, SWITZERLAND
Dr. W.L. Walse, Nat'l Bur Stand, USA
Dr. W.M. Stacey, Georg Inst Tech, USA
Dr. S.T. Wu, Univ Alabama, USA
Mr. Norman L. Oleson, Univ S Florida, USA
Dr. Benjamin Ma, Iowa State Univ, USA
Magne Kristiansen, Texas Tech Univ, USA
Dr. Raymond Askew, Auburn Univ, USA
Dr. V.T. Tolok, Kharkov Phys Tech Ins, USSR
Dr. D.D. Ryutov, Siberian Acad Sci, USSR
Dr. M.S. Rabinovich, Lebedev Physical Inst, USSR
Dr. G.A. Eliseev, Kurchatov Institute, USSR
Dr. V.A. Glukhikh, Inst Electro-Physical, USSR
Prof. T.J. Boyd, Univ College N Wales, WALES
Dr. K. Schindler, Ruhr Universitat, W. GERMANY
Nuclear Res Estab, Julich Ltd, W. GERMANY
Librarian, Max-Planck Institut, W. GERMANY
Dr. H.J. Kaeppler, University Stuttgart, W. GERMANY
Bibliothek, Inst Plasmaforschung, W. GERMANY